RSC Advances

PAPER

Cite this: *RSC Adv.*, 2014, **4**, 40686

Enhanced capacitance of rectangular-sectioned polypyrrole microtubes as the electrode material for supercapacitors†

Jiangtao Feng,[a] Wei Lv,[a] Jianwei Liu,[a] Jingjing Li,[a] Honghui Yang,[a] Hao Xu*[a] and Wei Yan*[ab]

Received 29th July 2014
Accepted 18th August 2014

DOI: 10.1039/c4ra07750d

www.rsc.org/advances

Rectangular-sectioned polypyrrole microtubes (R-PPy) were synthesized in aqueous solution with β-cyclodextrin (β-CD)/I_2 inclusion compound and $FeCl_3$ by chemical oxidation. Field emission scanning electron microscopy (SEM), Fourier transform infrared spectroscopy (FT-IR) and X-ray diffraction (XRD) were used to characterize the formation and molecular structure of R-PPy. From the results of the characterization, Complexes of β-CD/I_2–Fe^{2+} acted as the soft-template during the synthesis process of rectangular-sectioned polypyrrole microtubes. Some I^- ions retained in the backbone of the as-prepared PPy served as the counter ions after rinsing. Furthermore, R-PPy demonstrated higher conductivity and better electrochemical properties than PPy particles synthesized by the conventional method (C-PPy). The specific capacitance of R-PPy (322.5 F g^{-1} at the current of 1 A g^{-1}) is almost twice as large as that of C-PPy. The original specific capacitance of R-PPy can be maintained at around 83.3% whereas it was only about 61.5% for the C-PPy after 2000 charge–discharge cycles. The larger specific capacitance and relatively high cycling stability of R-PPy make it a more attractive candidate for energy storage electrodes than C-PPy.

1. Introduction

In recent years, more and more interest has been focused on the application of clean energy and high power energy sources for the outstanding global energy and environmental issues. In this sense, supercapacitors, also known as electrochemical capacitors, have attracted considerable attention due to their higher power density than batteries and larger energy density than conventional capacitors.[1,2] However, the supercapacitors provide the lower specific energy than batteries and fuel cells, which greatly limits their application.[3] There would be wide applications for supercapacitors if their specific energy could be improved. One of the keys to improve the performance of the supercapacitors is to obtain the new electrode materials which can provide good energy store behavior.

Generally, the electrode materials for the supercapacitors can be divided into two types. One type of the electrode materials is carbon based matters, for instance active carbon, carbon nanotubes and graphene, which show electrical double layer capacitor.[4] Another main electrode materials for the supercapacitors are metal oxides like MnO_2, RuO_2 and NiO_2, and conducting polymers (CPs), such as polyaniline (PANI), polypyrrole (PPy). These two categories exhibit pseudocapacitance based on fast and reversible redox reaction or faradic charge transfer reaction. Conducting polymers are considered as the important electrode materials for their higher charge density than carbon materials and lower cost than metal oxides. Among the various CPs, PPy is considered as an appropriate electrode material for supercapacitors due to its intrinsic electrical conductivity, good environmental stability, biocompatibility and low cost. Additionally, PPy presents fast doping/de-doping process, which leads to the rapid charge exchange in the polymer chains.[5] However, the practical capacitance of PPy electrode is lower than the theoretical value because the inner layer of electrode cannot be fully used. Besides, PPy electrode is not sufficiently stable after long-time redox cycles, which has limited its application for the electrode material of supercapacitors.[6] In general, several strategies have been used to enhance the capacitor performance of PPy. One is depositing PPy on the porous materials, such as carbon nanotubes,[7,8] graphene[9,10] and carbon fibers,[11] metals,[12,13] metallic oxides[14,15] and other materials.[16,17] The other is preparing the novel morphology of PPy using different synthetic ways. For instance, the well-defined PPy nanowire arrays in homogenous was synthesized by an one-step electropolymerization. This PPy nanowire arrays presented a capacitance of 566 F g^{-1}, which was

[a]*Department of Environmental Science and Engineering, Xi'an Jiaotong University, Xi'an 710049, P.R. China. E-mail: xuhao@mail.xjtu.edu.cn; yanwei@mail.xjtu.edu.cn; Fax: +86-29-82664731*

[b]*State Key Laboratory of Multiphase Flow in Power Engineering, Xi'an Jiaotong University, Xi'an 710049, P.R. China*

† Electronic supplementary information (ESI) available. See DOI: 10.1039/c4ra07750d

better than that of PPy film at the same condition.[18] The nanowires of PPy on graphite rod were also prepared by electrochemical method and showed an area specific capacitance of 45.01 mF cm^{-1}.[19] However, the large-scale synthesis of the CPs is difficult by using the electropolymerization. On the other hand, PPy nanospheres were synthesized in glycerol medium by chemical polymerization. The specific capacitance of the PPy nanospheres was 200.3 F g^{-1}, which was larger than that of the conventional PPy synthesized in water (151.0 F g^{-1}).[20] Furthermore, more studies indicated that the capacitance performance of PPy as the supercapacitor electrode material was strongly affected by the morphology of this polymer.[21,22]

Cyclodestrins (CDs), a class of oligosaccharides including α-CD, β-CD, γ-CD and other derivatives, have widely been used to prepare a variety of PPy or PANi with different morphologies and promote the physicochemical properties for their special molecular structure.[23,24] In our previous report,[25] the PPy with hexagonal micro-sheet morphology, which presented good capacitance, was synthesized in the aqueous solution containing α-cyclodextrin/Acid Red G inclusion compounds and ferrous cations. In this study, the rectangular-sectioned polypyrrole microtubes synthesized in aqueous with β-cyclodextrin/I_2 inclusion compound were firstly used as the electrode material for supercapacitor and presented better supercapacitor performance than that of PPy particles prepared by conventional method.

2. Experimental section

2.1. Materials

Pyrrole monomer (98%) purchased from Qingquan Pharmaceutical & Chemical Ltd. (Zhejiang, China) was distilled under vacuum and kept in refrigerator under the protection of nitrogen before used. Iodine (I_2) and potassium iodide (KI) were purchased from Sinopharm Chemical Reagent Co., Ltd. (Shanghai, China) as analytical reagent. Beta-cyclodextrin (β-CD, biological grade) was supplied by Liquan Chemical Industry Company (Shaanxi, China). Ferric chloride hexahydrate ($FeCl_3 \cdot 6H_2O$, 98%) and ferrous chloride tetrahydrate ($FeCl_2 \cdot 4H_2O$, 98%) were got from Beijing Chemicals, ethanol (anhydrous, 99.8%, Sinopharm Chemical Reagent Co. Ltd, Shanghai, China), Carbon electrode (Aido Hengsheng Technolog Co. Ltd, Tianjing, China), polyvinylidenedifluoride (PVDF, China Bluestar Chengrand Chemical Co. Ltd), black carbon (super-P-Li) were used as-received.

2.2. Preparation of the rectangular-sectioned PPy microtubes

The rectangular-sectioned PPy microtubules were synthesized by the soft-template method in β-CD/I_2 inclusion compound aqueous using $FeCl_3$ as oxidant. The typical synthetic process is as follows. First, 3 mL KI–I_2 solution (12.7 g I_2 dissolved in 1000 mL 36 wt% KI solution) was added into β-CD solution (0.3 mmol β-CD was dissolved in 30 mL deionized water) and stirred for 30 min at ambient temperature. The filemot suspension was moved to a three-necked flask with mechanical stirring device and cooled to 5 °C in ice-water bath. Then, pyrrole monomer (0.17 g, 2.5 mmol) was added to the suspension. By stirred for 30 min, $FeCl_3$ solution (1.0 mol L^{-1}, 12 mL) was dropwise added into the mixture slowly within 120 min. After that, the polymerization process was continued another 24 h at 5 °C under static condition. Finally, the obtained black precipitate was washed with water and ethanol several times until the filtrate being colorless, followed by drying in vacuum oven at 50 °C for 24 h. The sample was labeled as R-PPy.

The synthesis route of conventional PPy particle (C-PPy) was similar with that of the R-PPy, except that no KI–I_2 and β-CD were added.

2.3. Preparation of supercapacitor electrode with PPy samples

The electrochemical properties of as-prepared PPy samples as the electrode material for supercapacitor were investigated. The working electrode was prepared by mixing 70 wt% active mass (PPy sample), 20 wt% carbon black as conducting agent, and 10 wt% binder (PVDF) stirring for 24 h under the condition of the ambient temperature. The as-prepared mixture of the three components was pasted onto the glassy carbon electrode and dried at 80 °C overnight in vacuum.

2.4. Characterization and electrochemical measurements

The morphologies were characterized by field emission scanning electron microscopy (FESEM, JSM-6700F, Japan). The conductivities of the samples were tested by the standard four-probe method at ambient temperature. Fourier transform infrared spectra (FT-IR) of samples were measured by the KBr pellet method on a BRUKER TENSOR 37 FT-IR spectrophotometer in the range of 4000–400 cm^{-1}. The elements of the samples were characterized in the X-ray fluorescence spectrometer (XRF, S4 PIONEER, Bruker, Germany). X-ray diffraction (XRD) patterns of the samples were obtained with an X'Pert PRO MRD Diffractometer using Cu-Kα radiation. The BET surface area (S_{BET}), total pore volume (V) and average pore radius (R) were measured at 77 K using Builder SSA-4200 (Beijing, China).

A three-electrode system was adapted to evaluate the electrochemical performance of the synthesized PPy samples. The mass loading for the active materials is around 1.0 mg cm^{-2} calculated with an Analysis balance (METTLER AE240). The electrochemical tests were conducted with a CHI 660D electrochemical workstation in 1.0 M H_2SO_4 aqueous solution with a three electrode cell where Pt foil serves as the counter electrode and Ag/AgCl electrode as the reference electrode.

3. Results and discussion

3.1. Characterizations of the samples

The morphology of PPy prepared in the KI–I_2 and β-CD system is rectangular-sectioned microtubes (Fig. 1a and b) which is similar to the report.[26] The cross-section side length of the tube is about 1.0 μm and the length of the tubes is more than 50 μm. However, the morphology of C-PPy particles prepared by

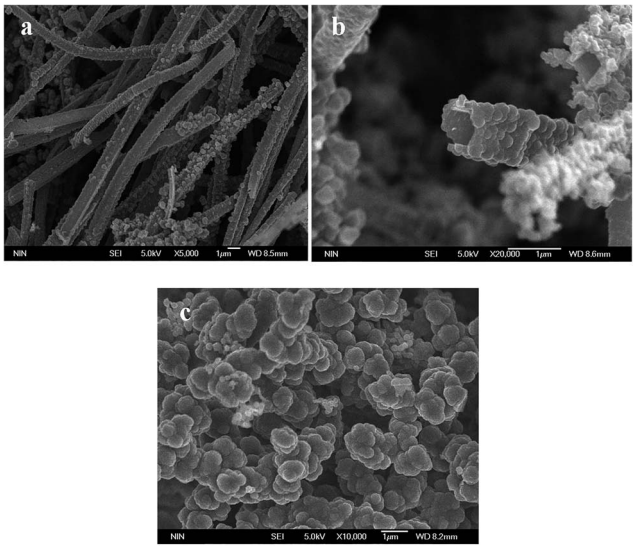

Fig. 1 SEM images of (a) a bundle of R-PPy microtubes; (b) a cross-section of the R-PPy microtube; (c) the cauliflower-like PPy particles prepared by conventional method.

conventional method is the traditional cauliflower, as shown in Fig. 1c.[27] This suggested that the KI–I_2 and β-CD system is the critical factor for the formation of R-PPy microtubes. The conductivities of the R-PPy and C-PPy are 43.7 S cm^{-1} and 7.14 S cm^{-1}, respectively.

The XRD patterns of samples in this study are shown in Fig. 2. The broad band from 20° to 30° at the patterns of R-PPy microtubes before and after rinse is identified to the amorphous PPy. However, The β-CD/I_2–Fe^{2+} complex exhibits distinct diffraction peaks at nearly $2\theta = 19.9°$, 22.6°, 30.3°, 33°and 34.9°, which are different from the diffraction of β-CD/I_2 inclusion compound. Meanwhile, there are still some relative sharp peaks (2θ = 22.6 and 33°) in the XRD pattern of R-PPy microtubes before rinse, corresponding to the same position of 2θ in the XRD patterns of β-CD/I_2–Fe^{2+}, which may indicate that some of the β-CD/I_2–Fe^{2+} complex could be in the as-prepared R-PPy structure. But after being rinsed these peaks become too small to be found, indicating that the β-CD/I_2–Fe^{2+} complex can be easily rinsed from the R-PPy microtubes. This is very similar to the literature.[28] The structures of the R-PPy microtubes and the C-PPy particles were also investigated by FT-IR spectroscopy (Fig. S1†). The band at 1545 cm^{-1} is considered as the C=C ring stretching for quinonoid structure in PPy, while the band at 1472 cm^{-1} is attributed to C–N stretching vibration in pyrrole ring. Additionally, it is believed that the bands at 1302, 1168 and 1039 cm^{-1} are ascribed to on-plane vibration of =C–H, and the band at 893 cm^{-1} is for =C–H out-of-plane vibration, respectively.[29–31] This indicated that the backbone of the PPy prepared in the KI–I_2 and β-CD system is the same as that of PPy prepared by conventional route.

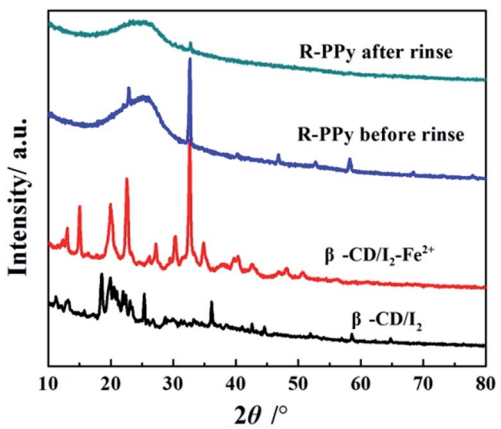

Fig. 2 XRD patterns of samples.

On the other hand, the present of β-CD will impact the X-ray diffraction pattern and FT-IR spectrum of PPy. The X-ray diffraction pattern of PPy will exhibit crystallization peaks of β-CD when β-CD present, even the content of β-CD is little.[24] Furthermore, the characteristics of β-CD would also present in the FT-IR spectrum of PPy, and further result in the shift of the PPy peak position.[24,32] For example, the peaks at 1933 and 1638 cm^{-1}, as the characteristic of β-CD, would appear in the FT-IR spectrum of PPy.[33] Meanwhile, the peak positions of the R-PPy would also shift in its FT-IR spectrum if β-CD presents in PPy structure. In this study, there is no characteristic peak of β-CD in the FT-IR spectrum of R-PPy, and the peaks of R-PPy do not shift. The X-ray diffraction pattern of R-PPy rinsed exhibits only a broad peak from 20° to 30°, which indicates the amorphous structure of R-PPy. These evidences all indicate the absence of β-CD in R-PPy and the almost pure R-PPy microtubes were prepared.

3.2. Formation mechanism of R-PPy microtubes

The SEM and XRF of corresponding samples were used to comprehend the formation mechanism of R-PPy microtubes. The SEM images of β-CD/I_2–Fe^{2+} and β-CD/I_2–Fe^{3+} complexes are displayed in Fig. 3. The morphology of β-CD/I_2–Fe^{3+} shows a large number of rod-like material bundles together to form block, which is very different from the morphology of R-PPy microtubes. Meanwhile, PPy microparticles were synthesized in the same aqueous solution, in which APS was used as the oxidant instead of $FeCl_3$ (Fig. S2†). It is obviously noticed that the β-CD/I_2–Fe^{2+} complex reveals the rectangular-sectioned structure which is similar to the R-PPy microtubes. The complexes formed between Fe^{m+} and the inclusion compounds

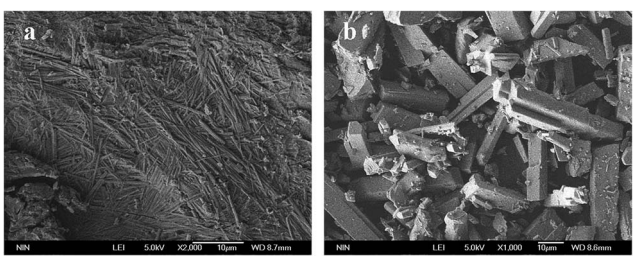

Fig. 3 SEM images of (a) β-CD/I_2–Fe^{3+} complexes; (b) β-CD/I_2–Fe^{2+} complexes.

of cyclodextrins were reported in some literatures.[28,34] In the literatures, the complexes of the Fe^{2+} and the inclusion compounds are considered as the soft-template. The PPy with novel morphologies were believed to grow up to the structure of the complex and along this trend. Meanwhile, β-CD can impact the molecular structure of conducting polymer,[35] and further lead to the different morphologies of conducting polymer.[36] To understand this procedure, the XRF characterizations of the β-CD/I_2 inclusion compound, β-CD/I_2–Fe^{2+} complex, R-PPy microtubes before and after rinse were also performed. XRF data (Table 1) present the changes of the main elements in the synthesis process of R-PPy. As the oxidant and the coordination atom (Fe^{3+}), the content of Fe increases firstly and then decreases. The content of Fe in β-CD/I_2 inclusion compound is almost zero (0.0564 wt%), while it is 34.4 wt% in β-CD/I_2–Fe^{2+} and 0.789 wt% in R-PPy microtubes before rinse. After rinse, this date decreases to near zero (0.0416 wt%) again. The change trend of chlorine element in the samples experiences the same as that of Fe. The content of iodine (from KI–I_2 solution) decreases from 59.5 wt% in β-CD/I_2 inclusion compound to nearly 19.1 wt% in the R-PPy microtubes after rinse. Meanwhile, the content of K experienced the same process from nearly 9.87 wt% in β-CD/I_2 inclusion compound to 0.031 wt% in the R-PPy microtubes after rinse. From these evidences, the contents of the ions in PPy matrix decreased after the PPy sample is rinsed. The decrease of Fe and I reveals that R-PPy microtubes contains a certain number of β-CD/I_2–Fe^{2+}, which can be rinsed from the synthesized PPy and some of I^- was still stay in PPy matrix as the counter ion. All of these evidences indicate that the β-CD/I_2–Fe^{2+} complex play the initial model during the synthetic process of R-PPy microtubes. It means that I^- is not only as a part of the soft-model in the synthesis process of R-PPy microtubes, but also as the counter ion in the as-prepared R-PPy matrix.

Therefore, the formation process of the R-PPy microtubes (Fig. 4) is presumed as following: β-CD and I_2 were stirred in aqueous solution to form inclusion compounds firstly. After adding pyrrole and vigorous stirring the intensive mixture of β-CD/I_2 inclusion compounds and small pyrrole droplets were obtained. And then, the PPy with incompact wrapping around the β-CD/I_2 inclusion compounds was formed by the accession of $FeCl_3$. With the reaction carrying on, more and more Fe^{3+} was reduced to Fe^{2+}, which induces the formation of the β-CD/I_2–Fe^{2+} complexes. Moreover, β-CD/I_2–Fe^{2+} complexes were easily to emerge rectangular-section bar structure as appearance of the SEM image in Fig. 3. The PPy formed around the β-CD/I_2–Fe^{2+} complexes with the rectangular-section bar structure in the initial process and elongate along the direction of β-CD/I_2–Fe^{2+} complexes to establish microtube morphology. Furthermore, the β-CD/I_2–Fe^{2+} complexes can be eluted from the formed PPy in the rinse process which was well proved by the data of XRF and XRD.

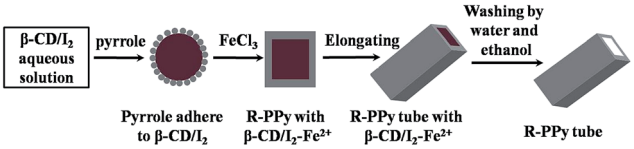

Fig. 4 The potential formation mechanism of the R-PPy microtubes.

Table 1 The results of XRF for samples

Samples	Amounts of elements/(wt)%			
	Fe	Cl	I	K
β-CD/I_2 inclusion compounds	0.0564	0	59.5	9.87
β-CD/I_2–Fe^{2+} complexes	34.4	0.327	33.8	1.15
R-PPy tubules before rinse	0.798	1.97	25.9	0.411
R-PPy tubules after rinse	0.0416	0.0233	19.1	0.031

3.3. Electrochemical properties

Cyclic voltammograms (CV) and galvanostatic charge–discharge technique in three-electrode system were used to test the electrochemical performance of the samples as the electrode material. Fig. 5 shows the CV curves of R-PPy and C-PPy as the electrode material in 1.0 M H_2SO_4 aqueous solution with a potential range of −0.4 to 0.6 V (*vs.* Ag/AgCl) in different scan rate from 20 to 100 mV s^{-1}. It can be seen that both CV curves of the samples have a peak near 0.0 V. Commonly, PPy, which contains counterions such as SO_4^{2-}, Cl^- and ClO_4^{2-}, can exhibit anion exchange behavior with other small anions for the mobility of these ions in the matrix.[37,38] In this study, the PPy samples were doped with Cl^- and I^-, while the electrochemical properties were carried out in H_2SO_4 aqueous solution. So, the peak of the ion exchange presents in the CV curves distinctly. Moreover, the CV curves of the R-PPy exhibit better supercapacitor behavior than that of C-PPy, for the areas encircled by the CV curve of R-PPy are much more like a rectangle, especially the curve in the scan rate of 100 mV s^{-1} (Fig. S3†). The phenomena are also testified by the galvanostatic charge–discharge technique. Fig. 6 shows the galvanostatic charging–discharging (GCD) curves of the PPy samples at different current ranging from 1 to 20 A g^{-1}. The specific capacitance is calculated as follows:

$$C_m = \frac{I \times \Delta t}{\Delta V \times m}$$

where C_m (F g^{-1}) is the specific capacitance, I (A) is the discharge current, Δt (s) is the discharge time, ΔV (V) is the potential range during discharge progress and m (g) is the mass of the PPy sample in the electrode.

It can be seen from Fig. 7 that the specific capacitances of R-PPy are 322.5, 237.6, 183.1, 150.8, 120.5 and 95.3 F g^{-1} at discharge current densities of 1, 2, 5, 10, 15 and 20 A g^{-1}, respectively. But the C-PPy exhibits the specific capacitances of 171.2, 151.7, 115, 86.7, 75 and 70 F g^{-1} in different current densities. It can be noted that R-PPy as electrode material has relatively better specific capacitance at the same current density in the range of 1 to 20 A g^{-1}, which is important for the electrode for a supercapacitor to provide high power density.[39] Meanwhile, the conductivity of the conducting polymer would relate to its specific capacitance and the larger conductivity will

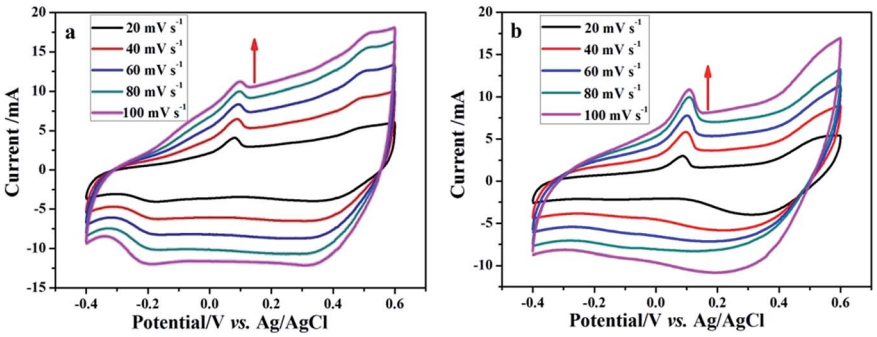

Fig. 5 Cyclic voltammetric of R-PPy microtubes electrode (a) and C-PPy particles electrode (b) in different scan rates.

result in higher specific capacitance.[40] The higher specific capacitances of R-PPy in different current densities agree well with its larger conductivity.

The nitrogen adsorption/desorption isotherms (Fig. S4a†) and Barrett–Joyner–Halenda (BJH) pore size distributions (Fig. S4b†) were also characterized to understand the capacitance behaviors of these two samples. The Brunauer–Emmett–Teller (BET) specific surface areas of R-PPy microtubes and C-PPy particles are calculated to be 64.1 $m^2 g^{-1}$ and 12.6 $m^2 g^{-1}$, respectively. It can also be observed that the majority of pores for two samples have a size in the range of 2–10 nm. The specific volume of R-PPy microtubes is relative higher than that of C-PPy particles. The larger specific surface area and specific volume of R-PPy microtubes may result in the better capacitance performance.

The cyclic stability of R-PPy and C-PPy were recorded up to 2000 cycles at a current density of 10 A g^{-1} in 1.0 M H_2SO_4 aqueous solution. The change of the specific capacitance for samples against the cycle number is shown in Fig. 8. It is noted that the specific capacitances of both samples decrease along with the cycles going. Around 83.3% of the initial capacitance can be maintained for R-PPy whereas only about 61.5% of that for C-PPy after 2000 cycles. Actually, there is a relative rapid decrease in specific capacitance to 14.44% for R-PPy after 1000 cycles. For C-PPy, this value is up to 36.54%. There is only about 2% loss observed in specific capacitance for both samples at the last 1000 cycles. This indicates that the specific capacitances of the samples as the electrode material are fairly constant after

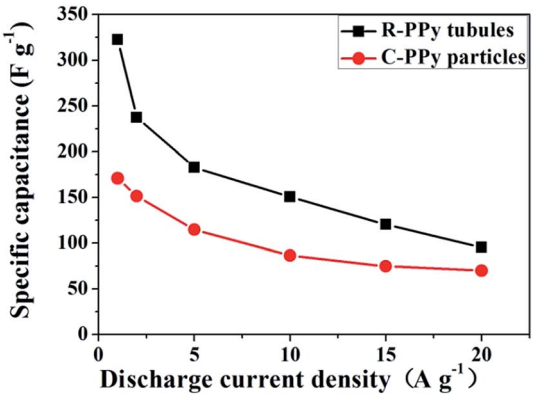

Fig. 7 Average specific capacitances of PPy electrodes at different current densities of 1, 2, 5, 10, 15, 20 A g^{-1}.

1000 cycles. Therefore, the larger specific capacitance, better rate capability and relatively higher cycling stability for R-PPy than that of C-PPy suggests that R-PPy is a more promising electrode material in energy storage than C-PPy. The R-PPy microtubes possess larger specific capacitance and higher cycling stability than the C-PPy. But C-PPy displays higher specific capacitance retention with increasing current densities from 1 to 20 A g^{-1} than R-PPy. The different trends of these performances are similar to the reports.[18,41] Therefore, R-PPy is a more promising electrode material in energy storage than C-PPy.

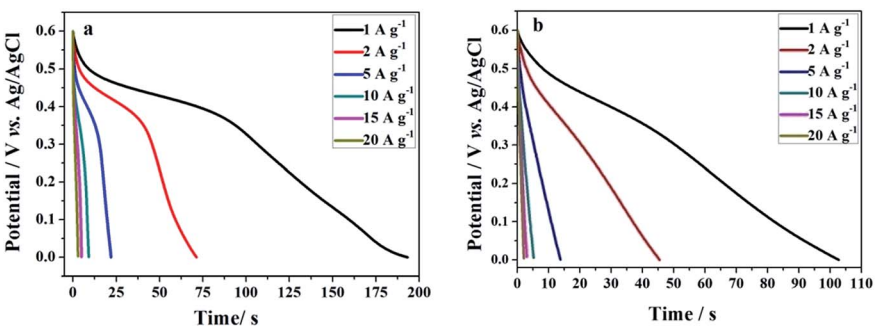

Fig. 6 Galvanostatic discharge profiles of (a) R-PPy microtubes and (b) C-PPy particles electrodes at different current densities.

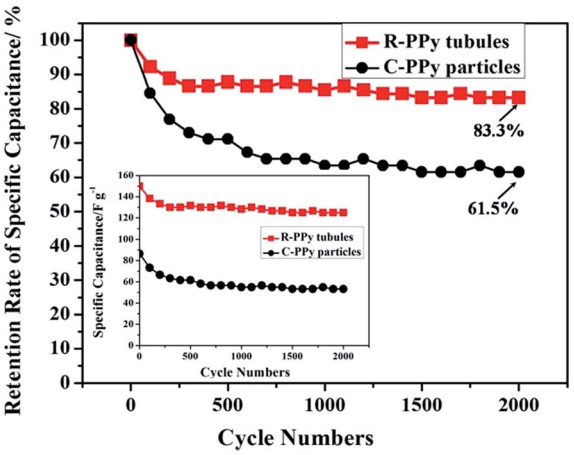

Fig. 8 Average specific capacitance retention *versus* cycle number of PPy electrodes at a current density of 10 A g^{-1} (insert is the specific capacitances *versus* cycle number of PPy electrodes at a current density of 10 A g^{-1}).

4. Conclusions

In this study, the rectangular-sectioned polypyrrole microtubes (R-PPy) were synthesized in the aqueous solution containing β-CD/I_2 inclusion compound. The characterizations of SEM, XRD and XRF testified that the β-CD/I_2–Fe^{2+} complexes were believed as the soft-template during the formation of the R-PPy microtubes. Meanwhile, the R-PPy microtubes as the electrode material for the supercapacitors displayed the larger specific capacitance than that of C-PPy. Moreover, the initial specific capacitance of R-PPy can be maintained around 83.3% whereas only about 61.5% of that for C-PPy after 2000 galvanostatic charge–discharge cycles. The synthesized R-PPy with improved specific capacitance performance is interest and may be applied to develop the high performance supercapacitors in large-scale.

Acknowledgements

The authors gratefully acknowledge the financial supports from the National Natural Science Foundation of China (Grant no.21307098), the Fundamental Research Funds for the Central Universities of China and China Postdoctoral Science Foundation (2013M532053).

References

1 G. H. Yu, L. B. Hu, M. Vosgueritchian, H. L. Wang, X. Xie, J. R. McDonough, X. Cui, Y. Cui and Z. N. Bao, *Nano Lett.*, 2011, **11**, 2905–2911.
2 L. L. Zhang and X. S. Shao, *Chem. Soc. Rev.*, 2009, **38**, 2520–2531.
3 R. A. Davoglio, S. R. Biaggio, N. Bocchi and R. C. Romeu-Filho, *Electrochim. Acta*, 2013, **93**, 93–100.
4 D. S. Patil, S. A. Pawar, R. S. Decan, M. G. Gang, Y. R. Ma, J. H. Kim and P. S. Patil, *Electrochim. Acta*, 2013, **105**, 569–577.
5 R. A. Davoglio, S. R. Biaggio, R. C. Romeu-Filho and N. Bocchi, *J. Power Sources*, 2010, **195**, 2924–2927.
6 L. Nyholm, G. Nyström, A. Mihranyan and M. StrØmme, *Adv. Mater.*, 2011, **23**, 3751–3769.
7 X. Lin and Y. Xu, *Electrochim. Acta*, 2008, **53**, 4990–4997.
8 K. Y. Shi and I. Zhitomirsky, *ACS Appl. Mater. Interfaces*, 2014, **5**, 13161–13170.
9 Y. Zhao, J. Liu, Y. Hu, H. H. Chen, C. G. Hu, C. C. Jiang, L. Jiang, A. Y. Cao and L. T. Qu, *Adv. Mater.*, 2013, **25**, 591–595.
10 X. Wang, C. Yang, H. D. Li and P. Liu, *Electrochim. Acta*, 2013, **111**, 729–737.
11 C. Y. Yang, J. L. Shen, C. Y. Wang, H. J. Fei, H. Bao and G. C. Wang, *J. Mater. Chem. A*, 2014, **2**, 1458–1464.
12 K. Shi, Y. Su and I. Zhitomirsky, *Mater. Lett.*, 2013, **96**, 135–138.
13 J. T. Wei, G. Z. Xing, L. Gao, H. Suo, X. P. He, C. Zhao, S. Li and S. X. Xing, *New J. Chem.*, 2013, **37**, 337–341.
14 A. Bahloul, B. Nessark, E. Briot, H. Groult, A. Mauger, K. Zaghib and C. M. Julien, *J. Power Sources*, 2013, **240**, 267–272.
15 Z. H. Dong, Y. L. Wei, W. Shi and G. A. Zhang, *Mater. Chem. Phys.*, 2011, **131**, 529–534.
16 X. Zhang, X. Z. Zeng, M. Yang and Y. X. Qi, *ACS Appl. Mater. Interfaces*, 2014, **6**, 1125–1130.
17 B. B. Yue, C. Y. Wang, X. Ding and G. G. Wallace, *Electrochim. Acta*, 2013, **113**, 17–22.
18 J. Y. Huang, K. Wang and Z. X. Wei, *J. Mater. Chem.*, 2010, **20**, 1117–1121.
19 H. R. Zhang, J. X. Wang, Q. J. Shan, Z. Wan and S. C. Wang, *Electrochim. Acta*, 2013, **90**, 535–541.
20 F. Ghamouss, A. Brugere, A. C. Anbalagan, B. Schmaltz, E. Luais and F. Tran-Van, *Synth. Met.*, 2013, **168**, 9–15.
21 H. Fu, Z. J. Du, W. Zou, H. Q. Li and C. Zhang, *J. Mater. Chem. A*, 2013, **1**, 14943–14950.
22 H. R. Ghenaatian, M. F. Mousavi and M. S. Tahmanfar, *Electrochim. Acta*, 2012, **78**, 212–222.
23 U. Tamer, C. Kanbes, H. Torul and N. Ertas, *React. Funct. Polym.*, 2011, **71**, 933–937.
24 S. M. Shang, W. Zeng and X. M. Tao, *RSC Adv.*, 2012, **2**, 4675–4682.
25 J. T. Feng, W. Yan and J. W. Zhu, *Synth. Met.*, 2010, **160**, 939–945.
26 J. Han, W. Yan and Y. B. Xu, *Chem. Lett.*, 2006, **35**, 306–307.
27 T. C. Wen, S. L. Hung and M. Diger, *Synth. Met.*, 2011, **118**, 11–18.
28 W. Yan and J. Han, *Polymer*, 2007, **48**, 6782–6790.
29 J. Liu and M. X. Wan, *J. Polym. Sci., Part A: Polym. Chem.*, 2001, **39**, 997–1004.
30 H. N. M. E. Mahmud, A. Kassim, Z. Zainal and W. M. M. Yunus, *J. Appl. Polym. Sci.*, 2006, **100**, 4107–4113.
31 J. Y. Jin, T. Ando, N. Teramae and H. Haraguchi, *Bunseki Kagaku*, 1991, **40**, 799–804.
32 Z. J. Gu, J. R. Ye, W. Song and Q. Shen, *Mater. Lett.*, 2014, **121**, 12–14.
33 M. Grigoras and D. G. Conduruta, *J. Inclusion Phenom. Macrocyclic Chem.*, 2006, **54**, 101–107.

34 X. Q. Hu, Y. Lu and J. H. Liu, *Macromol. Rapid Commun.*, 2004, **25**, 1117–1120.
35 Y. Hasegawa, Y. Inoue, K. Deguchi, S. Ohki, M. Tansho, T. Shimizu and K. Yazawa, *J. Phys. Chem. B*, 2012, **116**, 1758–1764.
36 Y. J. Ding, T. Adsiryim, S. Y. An and I. Nurulla, *J. Appl. Polym. Sci.*, 2008, **107**, 3864–6870.
37 X. Du, X. G. Hao, Z. W. Wang, X. L. Ma, G. Q. Guan, A. Abuliti, G. H. Ma and S. B. Liu, *Synth. Met.*, 2013, **175**, 138–145.
38 C. Weidlich, K. M. Mangold and K. Juttner, *Electrochim. Acta*, 2005, **153**, 1547–1552.
39 X. Peng, K. Huo, J. Fu, X. Zhang, B. Gao and P. K. Chu, *Chem. Commun.*, 2013, **49**, 10172–10174.
40 C. Yang and P. Liu, *Synth. Met.*, 2010, **160**, 768–773.
41 S. S. Shinde, G. S. Gund, D. P. Dubal, S. B. Jambure and C. D. Lokhande, *Electrochim. Acta*, 2014, **119**, 1–10.